THE JOURNAL OF PHYSICAL CHEMISTRY B

B: Fluid Interfaces, Colloids, Polymers, Soft Matter, Surfactants, and Glassy Materials

Water-Responsive and Mechanically-Adaptive Natural Rubber Composites by in-Situ Modification of Mineral Filler Structures

Shib Shankar Banerjee, Sakrit Hait, Tamil Selvan Natarajan, Sven Wiessner, Klaus Werner Stöckelhuber, Dieter Jehnichen, Andreas Janke, Dieter Fischer, Gert Heinrich, James J.C. Busfield, and Amit Das

J. Phys. Chem. B, **Just Accepted Manuscript** • DOI: 10.1021/acs.jpcb.9b02125 • Publication Date (Web): 24 May 2019

Water-Responsive and Mechanically-Adaptive Natural Rubber Composites by In-Situ Modification of Mineral Filler Structures

Shib Shankar Banerjee[1], Sakrit Hait[1,2], Tamil Selvan Natarajan[1,2], Sven Wießner[1,2], Klaus Werner Stöckelhuber[1], Dieter Jehnichen[1], Andreas Janke[1], Dieter Fischer[1], Gert Heinrich[1,3], James Busfield[4], Amit Das[1,5*]

[1]Leibniz-Institut für Polymerforschung Dresden e. V., Hohe Straße 6, D-01069 Dresden, Germany
[2]Technische Universität Dresden, Institut für Werkstoffwissenschaft, D-01069 Dresden, Germany
[3]Technische Universität Dresden, Institut für Textilmaschinen und Textile Hochleistungswerkstofftechnik, D-01062 Dresden, Germany
[4]The School of Engineering and Materials Science, Queen Mary University of London, Mile End Road, London E1 4NS, UK
[5]Tampere University of Technology, Korkeakoulunkatu 16, Fi-33101 Tampere, Finland

Abstract:

A new biomimetic stimuli-responsive adaptive elastomeric material, whose mechanical properties are altered by a water treatment is reported in this paper. This material is a calcium sulphate ($CaSO_4$) filled composite with an epoxidized natural rubber (ENR) matrix. By exploiting the various different phase transformation processes that arise when the $CaSO_4$ is hydrated, several different crystal structures of $CaSO_4 \cdot x\ H_2O$ can be developed in the crosslinked ENR matrix. Significant improvements in the mechanical and thermal properties are then observed in the water treated composites. When compared with the untreated sample, there is approximately a 100 % increase in the dynamic modulus. The thermal stability of the composites is also improved by increasing the maximum degradation rate temperature by about 20 °C. This change in behaviour results from an *in-situ* development of hydrated crystal structures of the nano-sized $CaSO_4$ particles in the ENR matrix which has been verified using Raman spectroscopy, transmission electron microscopy, atomic force microscopy and X-ray scattering. This work provides a promising and relatively simple pathway for the development of next generation mechanically-adaptive elastomeric materials by an eco-friendly route which may eventually also be developed into an innovative biodegradable and biocompatible smart polymeric material.

Corresponding author email: das@ipfdd.de

Present address of Shib Shankar Banerjee is Nanomanufacturing Center, University of Massachusetts Lowell, MA 01854, USA

Introduction

Mechano-adaptive composites are a class of stimuli-responsive materials that can reversibly change their mechanical properties when exposed to an external stimuli such as a specific chemical, heat, light or an electro-magnetic field[1-2]. These composites present the next generation of smart materials for technological applications and the topic is receiving significant attention from scientists. However, there remain significant challenges when attempting to introduce adaptive mechanical properties in soft elastomeric systems. For example, one of the ongoing challenges in the tire industry is to design tires that can dynamically and reversibly adapt to specific driving conditions. It is anticipated that the development of a mechano-adaptive tire could be a solution. In nature mechanical adaptability is a very common, for example, sea cucumbers can reversibly alter the stiffness of their dermis[1-2]. Inspired from such biological systems, research into mechano-adaptive soft materials is increasing and this has shown potential interest in a variety of different fields[3-7]. Recently, the elucidation of specific molecular mechanisms within natural materials that can present adaptive features has provoked the development of many biomimetic adaptive materials which can mimic their architecture and function upon command[8-13]. Among the different classes of polymeric materials, elastomers are the most fascinating because of their significant large strain elasticity. For particulate reinforced elastomeric composites, in addition to the intrinsic mechanical properties that originate from the elastomer matrix, the interactions between the rubber and the filler as well as the interactions between the filler particles also play a significant role in determining the resulting mechanical behaviour. Therefore, any external stimuli such as a change in the temperature or electric field or a change in the concentration of the solvents or the ions present at the interface that can alter the rubber-filler interactions can also trigger a change in the mechanical properties of the composite.

Calcium sulphate ($CaSO_4$) is already used as a particulate filler material in some polymer products[14-16]. This naturally occurring mineral can form different crystals structures according to their degree of hydration, such as anhydrite ($CaSO_4$), hemihydrate/bassanite ($CaSO_4$ 0.5 H_2O) and gypsum ($CaSO_4 \cdot 2\ H_2O$)[17-18]. Calcium sulphate occurs naturally in evaporate deposits in various hydrated forms including anhydrite, plaster of Paris and gypsum. Clearly these are important materials for the building and construction industries. Generally, the conversion of these phases into each other takes place by a hydration / dehydration process. Dehydration of gypsum at elevated temperatures yields hemihydrates (α,β) with different thermal and hydration characteristics. Conversely, hemihydrate and anhydrite can be rapidly converted to gypsum by a hydration process. However, the detailed crystal structure development during the hydration-dehydration process of the $CaSO_4/H_2O$ system depends on various parameters such as time, temperature or rate of crystallization. In order to fulfil different applications, the size and shape of calcium sulphate crystals has to be controlled. Therefore, there is the potential for the *in-situ* development of several different crystal structures of $CaSO_4$ when incorporated into a polymer matrix. However, it is a real challenge to grow specific crystal structures inside a hydrophobic polymer matrix resulting either from a constriction on the available volume or a limit on the water absorption capacity of the hydrophobic polymer. By exploiting the multiple phase transformation processes of the $CaSO_4/H_2O$ system, as described above, a novel strategy can be devised to develop biomimetic water-responsive natural elastomer composites which possess adaptive mechanical properties. The stiffness of these composites can be altered to reflect different requirements under specific conditions. There are a few reports in the literature on the adaptive characteristics of the elastomers using natural materials such as cellulose whiskers or cement.[19-21] However, the naturally abundant and industrially important mineral, $CaSO_4$ has not yet been widely explored as an adaptive filler materials[22]. In this research, *in-situ* hydrated crystal structures of $CaSO_4$ in an epoxidized natural rubber (ENR) matrix were developed

from its metastable hemihydrate phase. The *in-situ* morphological transformation of $CaSO_4$ from the hemihydrate to other stable hydrates leads to significant increases in the mechanical and thermal performance of the resulting elastomeric composites. As water plays a significant role in the phase transformation processes, the elastomer must exhibit some hydrophilic behaviour. However, the uptake of water by general purpose elastomers is very limited. Different strategies are therefore required to increase the hydrophilic characteristics of the elastomer matrix in the composites[10, 13, 21, 23]. Resulting from the presence of the epoxy group, epoxidized natural rubber (ENR) can absorb a significantly greater amount of water. In this work, effort was made to promote *in-situ* hydration of $CaSO_4$ within the ENR matrix. Several analytical methods, such as Raman spectroscopy, transmission electron microscopy, atomic force microscopy and X-ray scattering were used to verify the various different states of the phase transformation processes. A simple methodological approach allows a mechanistic understanding of water-responsive ENR-$CaSO_4$ composites to be developed which will potentially result in the development of a new generation of mechanically adaptive polymeric materials.

Experimental

Materials:

Epoxidized natural rubber (ENR) having 50 mol% epoxidic units, with a density 1.02 g/cc and Mooney viscosity ($ML_{(1+4)}$, 100°C) 80 was procured from Weber and Schaer, GmbH, Germany.

The vulcanizing accelerator N-tert-butyl-2-benzothiazyl sulphonamide (TBBS) was obtained from Rhein Chemie Rheinau, Mannheim, Germany. Industrial grades of sulphur (S) and zinc oxide (ZnO) were also used in this study. Calcium sulphate ($CaSO_4$) (99 % anhydrous) was supplied from Acros Organics, Geel, Belgium. At room temperature the commercial $CaSO_4$

was present at a hemihydrate form, whereas, anhydrous $CaSO_4$ was dehydrated at 150-200 °C. The hydrated $CaSO_4$ was also prepared by treating commercial $CaSO_4$ with water.

Preparation and characterization of composites:

The compounding of ENR with 50 phr $CaSO_4$ including other ingredients such as the cure package including S, ZnO and TBBS was done using a Haake Rheometer (Thermo Electron GmbH, Karlsruhe) at a 60 rpm rotor speed and 60 °C temperature for 10 min. After mixing in the Haake, the resulting compound were further mixed by a laboratory-sized two-roll mill (Poly-mix110L, friction ratio = 1:1.25, roll temperature = 40 °C) and finally the resulting rubber compound was collected as thick rubber sheets. The ENR samples were cured by a hot press at 150 °C until their optimum curing time (t_{c90}). This t_{c90} was obtained from a rheometric study using an oscillating die rheometer at 150 °C operating at a frequency of 1.67 Hz (SIS V-50, Scarabeus GmbH, Germany).

To measure the rate and extent of water uptake, crosslinked rubber samples were immersed in deionized water at room temperature and at 80 °C. The weight of the sample was measured as a function of time at various temperatures immediately after the removal of the surface water using tissue paper. The mass percentage of water absorption (M_t) with time (t) was obtained using the following equation[24]:

$$M_t = \frac{W_t - W_0}{W_0} \quad (1)$$

where W_0 is the initial weight and W_t is the weight at time t.

The various tensile tests on the elastomeric composites were done at room temperature using a Zwick mechanical test machine (Z010, Ulm, Germany) at a crosshead speed of 200 mm min^{-1}.

The dynamic mechanical analysis was performed in tension mode using an Eplexor 2000N dynamic measurement system (Gabo Qualimeter, Ahlden, Germany). Temperature dependent dynamic mechanical tests were carried out from -50 to +100 °C with heating rate of 2 K min^{-1} using an isochronal frequency of 10 Hz at a 0.5 % dynamic strain and 1 % static strain. Amplitude sweep measurements ('Payne effect') were undertaken at room temperature at a constant frequency of 10 Hz, using a static load at 60 % pre-strain and dynamic load of 0.01–30 %. To create a value for the 1000% strain (E'_{∞}) for use in a Kraus model[25] defined in equation 3 the modified Guth-Gold equation defined by equation 2 was used. This extrapolation is necessary to have stable modulus values in the rubbery plateau region. Frequency master curves were produced using time-temperature superposition (TTS) after measuring a combined frequency sweep experiments over a range of temperatures. The temperature ranges used were from -50 to 100 °C and the frequency range was from 0.5 to 30 Hz. The thermal degradation behaviour of the composites was investigated using a thermogravimetric analyser (TGA Q5000, TA instruments) using an inert nitrogen atmosphere. The experiment was carried out up to 800 °C and the heating rate was 5, 10 and 20 K min^{-1} respectively. The activation energy of the composites was calculated using the Kissinger method[26] as described in the supporting information.

The structural changes of calcium sulphate ($CaSO_4$) in the ENR matrix were investigated using transmission electron microscopy (TEM JEM 2010), atomic force microscopy (AFM, Bruker-Nano Inc., Santa Barbara, CA) Raman spectroscopy and XRD, respectively. The ultra-thin sections of the samples were prepared by ultramicrotomy (Leica Ultracut UCT) at -100 °C for use in the TEM and AFM analysis. The AFM experiments were conducted in a tapping mode at room temperature. Raman-spectra was measured using Confocal Raman Microscope alpha 300 R (WITec GmbH, Ulm, Germany) equipped with a laser with a 785 nm wavelength, and a laser power of 200 mW.

The X-ray scattering experiments (in symmetric transmission) were performed at room temperature by means of the 2-circle diffractometer XRD 3003 T/T (GE Sensing & Inspection Technologies / Seifert-FPM, Freiberg, Germany) using Cu-K_α radiation (monochromatization with a Göbel mirror). Scattering intensities were recorded in 2θ-range of 1 − 65° with steps $\Delta 2\theta = 0.05°$ and 40 s per step. Powder-like samples were filled in 1 mm glass tubes, other samples were wrapped in Al foil (samples thicknesses here were in the range of ~1.5 mm). Scattering patterns are presented as lg(I) vs. 2θ, resp. vs. lg(d) (with d-values derived using Bragg's law). The main reflections of crystalline phases were assigned using the crystallographic databank PDF-2 (ICDD, Newtown Square, Pennsylvania, USA).

Results and discussion

The water absorption tests revealed that ENR and ENR-$CaSO_4$ composites can absorb only a very limited 1 wt.% of water at room temperature (Figure S1a-b). Due to hydrophobic nature of the crosslinked sample the water absorption capability of the rubber is still poor. However, a significant improvement of the water uptake value was observed at the elevated temperature. It was revealed that ENR and ENR-$CaSO_4$ composites can absorb about 14 wt.% and 40 wt.%, respectively of water at 80 °C after 10 days of water treatment (See Figure S1). The effect of water absorption on the structure and properties of the composites were evaluated by various analytical methods. Once swollen, the unfilled ENR had no perceptible change of properties (See Figure S2).

The effects of water absorption on the mechanical and dynamic mechanical properties of the elastomer composites are reported in Figure 1a-e. Changes to the stiffness of the composite under different conditions is of significant interest therefore the storage modulus (E') of the different composites was measured. A significant increase in E′ was observed for the water treated sample in the rubbery plateau region when compared with the freshly prepared and untreated sample. (Figure 1b). For example, when tested at 30 °C, E' for the untreated sample

was 2.6 MPa which increased to 6.4 MPa after the water treatment. A significant reduction of the tan delta peak height value was also observed after hydration which probably resulted from a more restricted movement of the polymer chains by the calcium sulphate filler after hydration. (Figure 1c). In addition, a slight increase in the glass transition temperature of the composite was also observed after the water treatment process. Figure 1a shows the effect of water treatment on the tensile properties. Interestingly, the stress-strain curve of water-treated sample becomes stiffer when compared to the untreated sample. In accordance with the dynamic tests of the storage modulus, an approximately 100 % increase of the small strain Young's modulus of the composites was achieved after hydration. This observation directly indicates an improvement in the reinforcing characteristics of the water treated $CaSO_4$ particles. As the water treatment does not significantly alter any of the mechanical properties of the unfilled rubber, it is clear that the alteration of the mechanical performance of $CaSO_4$ filled composite is associated with changes to the polymer filler interactions or the filler structure and morphology. The enhanced mechanical and dynamic mechanical properties can be explained by assuming that either stronger rubber-filler interactions are developed as the filler is hydrated or that the filler geometry somehow develops a higher aspect ratio. Possibly, during the water treatment a structural change to the $CaSO_4$ particles takes place that creates a finer structure with a higher aspect ratio for the reinforcing particles. To explain this improved rubber filler interaction the following modified Guth-Gold equation was introduced[27-28].

$$E'/E'_0 = 1 + 2.5f\phi + 7.6f^2\phi^2 \qquad (2)$$

Where E' is the Young's modulus of the filled sample, E'_0 is the Young's modulus of the rubber sample without any filler), ϕ is the volume fraction of the $CaSO_4$ particles, and f is the aspect ratio or shape factor. Now, if we consider that the total filler volume fraction cannot be significantly changed by water treatment, however, a dramatic enhancement of E' is observed. This can be only explained by if the value of $f > 1$ is considered. This discussion directly implies that after water treatment the aspect ratio of the particles is also increased. Another

explanation behind the mechanical properties enhancement by water treatment can be also given. The density of calcium sulphate di-hydrate is 2.31 g/cm^3, whereas the density of hemi-hydrate is 2.62 g/cm^3 for beta form and 2.76 g/cm^3 for alpha form[22]. That means that the volume of the corresponding water treated (di-hydrate) form is higher than untreated (hemi-hydrate) form. This enhancement of the volume fraction could be one of the reasons of such mechanical properties alteration.

In order to understand the filler-filler interactions of the $CaSO_4$ filled ENR composite, dynamic strain sweep was performed and analyzed with a phenomenological model. The storage modulus was found to be independent of dynamic strain for the untreated sample, whereas, a strong nonlinear dependence of storage modulus as a function of dynamic strain was evident for the water treated sample (Figure 1d). This was attributed to destruction-reformation kinetics of a filler-network at low strains an effect that is often referred to as the Payne effect[29]. This effect is observed to a much greater extent on filled rubber samples when compared to unfilled or gum rubber samples. This strain dependence dynamic property, in present case the storage modulus, is explained using the agglomeration-de-agglomeration mechanism of the filler network in an elastomer matrix, which can be described using the Kraus model as defined using the following equation[25]:

$$\frac{E'(\gamma) - E'_\infty}{E'_0 - E'_\infty} = \frac{1}{1 + \left(\frac{\gamma}{\gamma_c}\right)^{2m}} \quad (3)$$

where, $E'(\gamma)$ is the storage modulus of the composite at a function of strain amplitude, γ. E'_∞ and E'_0 are the value of storage modulus at a very large strain and very low strain, respectively. γ_c and m are the critical strain and strain sensitivity parameter constant, respectively. At γ_c, the magnitude of $E'_0 - E'_\infty$ becomes half and its value is mainly dependent on the nature of the rubber or the filler and the degree of dispersion of the filler in a rubber

matrix. The value of *m* depends on specific fractal dimensions of the fractal agglomerate structures of the fillers and also the mechanism of the filler-filler contact breakage.[30] The values of γ_c are found to be significantly different at 0.8% and 49% for the untreated and water treated composites respectively. The *m* values are virtually identical at 0.63 and 0.60, for the untreated and water treated composites respectively. The lower value of γ_c for the untreated sample can be associated with a weak Payne effect where the behavior resembles that of a gum rubber without any filler. In present case the untreated calcium sulphate is acted as non-active filler and the reinforcing effect is negligible. In present case 50 phr calcium sulphates in untreated form remains under the critical percolation threshold and the filler-filler network is not established. However, after water treatment the density of the di-hydrate form becomes lower and the volume fraction of the filler becomes larger. This results a strong-filler filler network which is reflected in Payne effect. Furthermore, due to water treatment some adsorbed water molecule on the filler surface may form hydrogen bonding between two filler particles that can also enhance the filler-filler networks. Obviously, this indicates a significant change in either the specific nature of the rubber-filler or the filler-filler interactions in the treated composites when compared to the untreated one due to the formation of different hydration-induced phase morphological structures which is discussed later.

The water-induced reinforcement characteristic of the $CaSO_4$ particles has also been explored using the TTS derived modulus versus frequency master curves. Figure 1e shows the dynamic mechanical behaviour (E')of the composites over a wide range of frequencies. In the high frequency glassy region, the qualitative behaviour of E' was very similar for both the treated and the untreated samples. At intermediate frequencies, a power-law frequency behaviour $E'(\omega) \propto \omega^a$ with an exponent a = ½ was also found for both the samples. At lower frequencies E' for the elastomer networks tends towards a plateau modulus, E_{eq}. This E_{eq} was found to be higher for the treated composite (4.2 MPa) when compared to the untreated one (1.7 MPa). This

observation may be attributed to an additional reinforcing contribution of the hydrated $CaSO_4$ particles and a higher contribution from the filler network for the water-treated composite.

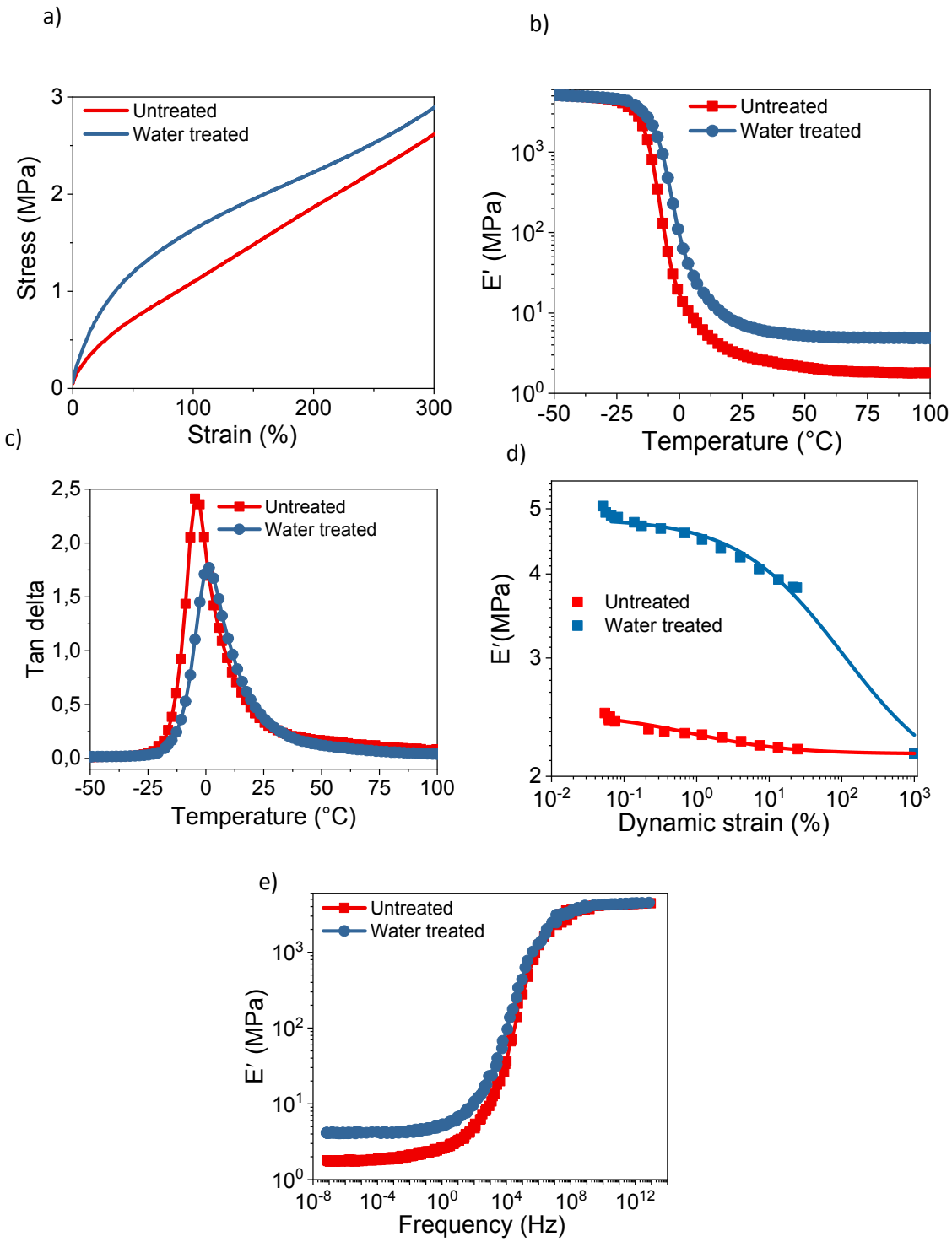

Figure 1. **Effect of hydration on the mechanical and dynamic mechanical properties of ENR- $CaSO_4$ composites: (a) tensile stress-strain plots, (b) storage modulus as a function of temperature, (c) loss tangent spectra as a function of temperature, (d) storage modulus as a function of dynamic strain (e) frequency sweep master curve of the untreated and treated ENR-$CaSO_4$ composites. Treated sample was prepared by immersing in water for 10 days at 80 °C. Then the sample was equilibrated for 72 hours at room temperature.**

In addition to changes in the mechanical behavior of the composites, significant change of the water-induced thermal stability was also found. The thermogravimetric analysis, as shown in Figure 2a-b, reveals an improved thermal stability of the hydrated sample. After hydration the maximum rate of thermal degradation after hydration was shifted to a higher temperature. For example, a 20 K shift in T_{max} was achieved after hydration compared to that of the untreated one. Figure 2c shows the kinetic analysis of the composites using Kissinger method[26]. The activation energy of the untreated sample was 135 kJ mol^{-1} which increased to 153 kJ mol^{-1} after hydration indicating a higher thermal stability of the more hydrated composites. The shift of T_{max} and a higher activation energy are probably associated with the morphological changes from the hemihydrate/anhydrite to hydrated crystal (gypsum) structure inside the ENR matrix. This crystal structure can produce a char which hinders the diffusion of volatiles and the mass transport required during decomposition which can delay the onset of degradation. The enhanced thermal stability of the water treated composite might be expected to result from the formation of nanoparticles or their enhanced interaction with the polymer network. Thus, there is an additional energy required to break the polymer-filler interactions prior to the onset of the polymer degradation. This observed improvement in the thermal stability suggests that $CaSO_4$ might be able to improve the thermal stability of rubber in an adaptive way.

Finally, Raman, TEM, AFM and X-ray data were used to observe the formation of hydrated crystalline structures inside the ENR matrix that are responsible for this increased mechanical, dynamic mechanical and thermal properties. This *in-situ* hydrated crystal structure of $CaSO_4$ in a confined elastomer matrix was analysed using Raman Spectroscopy. Prieto-Taboada *et al.* systematically analysed Raman spectra of each phase of the $CaSO_4/H_2O$ system and identified bands at 1008, 1015, 1025, 1017 and 1017 cm^{-1} for gypsum, bassanite, anhydrite III, anhydrite II and anhydrite I, respectively[31].

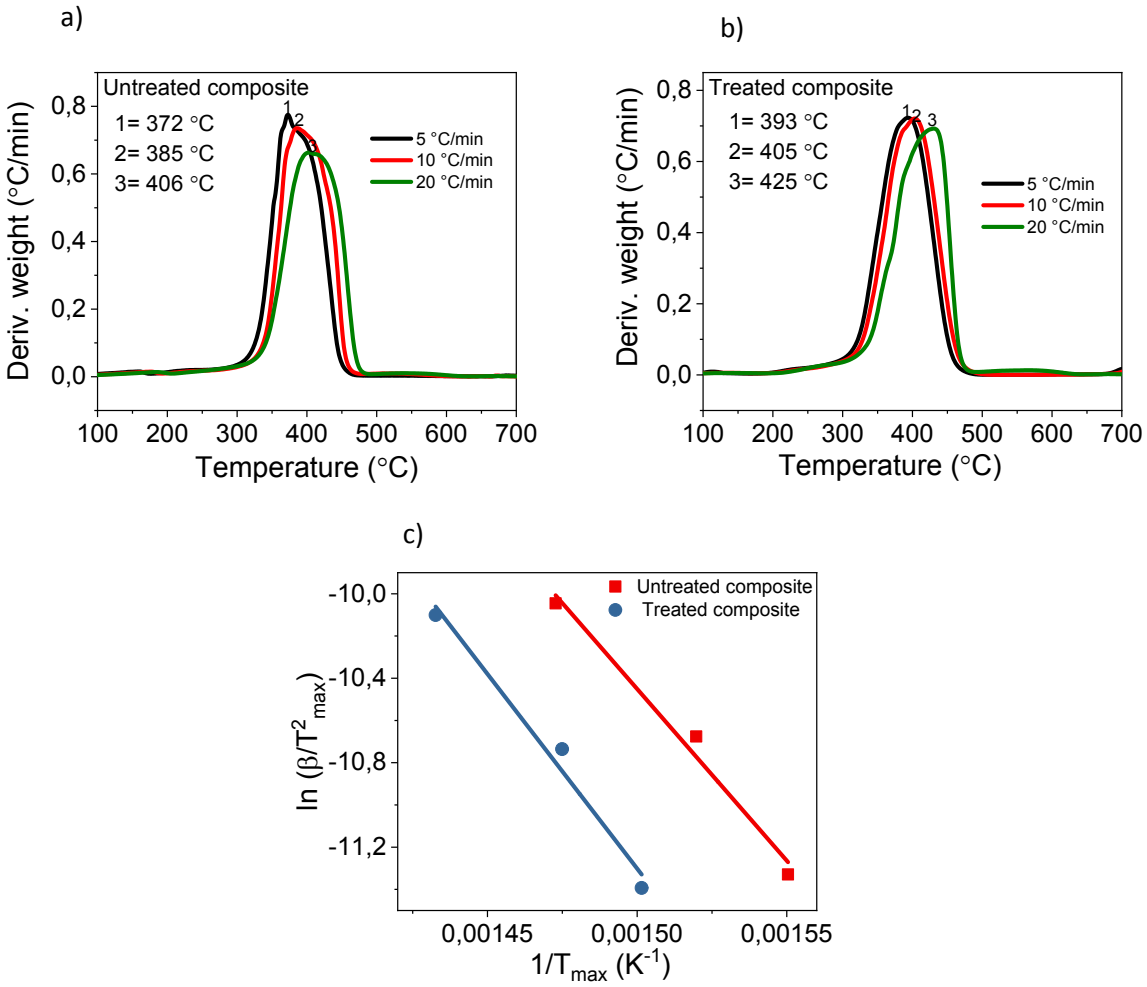

Figure 2. **Effect of hydration on thermal properties of ENR-$CaSO_4$ composites: TGA derivative weight vs. temperature of (a) untreated and (b) treated ENR-$CaSO_4$ composites, (c) Kissinger method applied to experimental TGA data on the untreated and treated composites at different heating rates (5, 10 and 20 K min^{-1} under nitrogen).**

As shown in Figure 3, the Raman bands of the commercial and water-treated $CaSO_4$ appeared at 1017 cm^{-1} and 1009 cm^{-1}, respectively. These bands correspond to the hemihydrate/anhydrite II/anhydrite I and gypsum, respectively. In the case of the untreated ENR-$CaSO_4$ composite, a single band at 1017 cm^{-1} was identified. Conversely, a major Raman band at 1009 cm^{-1} and a minor band at 1017 cm^{-1} were identified for the case of the water-treated sample. The appearance of both bands confirms the phase transformation process of hemihydrate to hydrate (gypsum) in the ENR matrix.

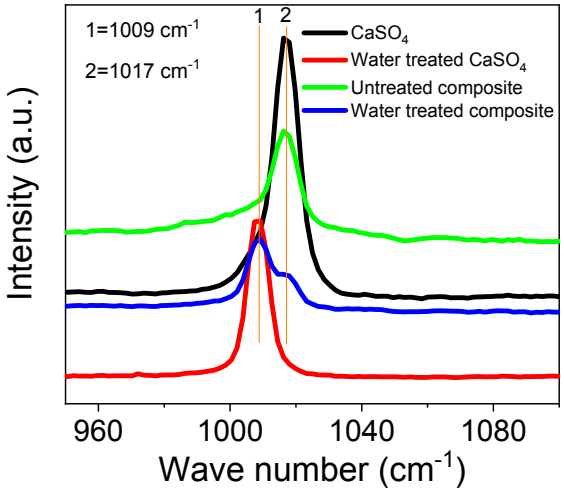

Figure 3. **Raman Spectroscopy of the commercial $CaSO_4$, water-treated $CaSO_4$, untreated and water-treated ENR-$CaSO_4$ composites.**

This phase transformation process has also been verified using XRD. Figure 4a shows a comparison of the scattering pattern. To recognize the crystalline phases, the main reflections were assigned by an acronym of the phase and their related Miller indices (hkl): A – anhydrite [$CaSO_4$], B – bassanite (hemihydrate) [$CaSO_4 \cdot 0.5\ H_2O$], G – gypsum [$CaSO_4 \cdot 2\ H_2O$], Z – zinc oxide [ZnO], and Al – aluminium (metal foil for preparation). Using XRD, a crystalline phase of sulphur was not easily observed. Untreated (dried) $CaSO_4$ contains bassanite and anhydrite (in comparable percentages), and a minor amount of amorphous phases ($2\theta_{max} \sim 26.5°$).

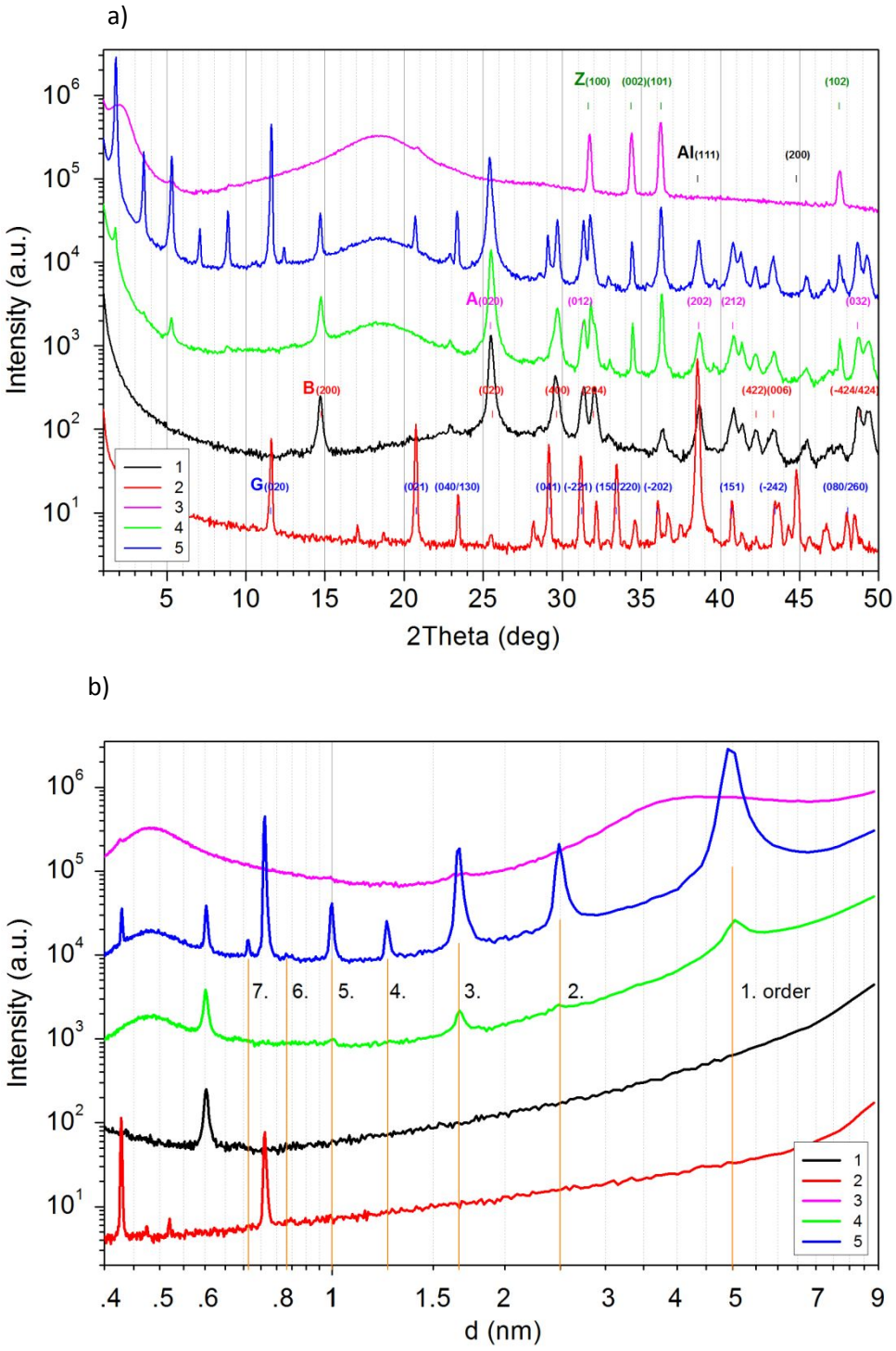

Figure **4. (a) XRD pattern [lg(*I*) vs. *2θ*] of dried $CaSO_4$, water-treated $CaSO_4$, cured ENR, untreated ENR-$CaSO_4$ composite and water-treated ENR-$CaSO_4$ composite. Abbreviations of reflections (hkl): A – anhydrite, B – bassanite, G – gypsum, Z – zinc oxide, Al – aluminium. Data shifted for better visualization; (b) XRD pattern [lg(*I*) vs. lg(*d*)] of dried $CaSO_4$ (1), water treated $CaSO_4$ (2), cured ENR (3), untreated ENR-$CaSO_4$ composite (4) and water-treated ENR-$CaSO_4$ composite (5). Data shifted for better visualization.**

After water treatment, both bassanite and anhydrite convert into gypsum (additionally a minor part of other unidentified crystalline phases, no amorphous scattering, and reflections from the wrapping aluminium foil used for this sample are observed). For better contrast to the composite samples the unfilled (cured) ENR is shown in Figure 4b. The XRD curve is characterized by a broad amorphous scattering maximum ($2\theta_{max} \sim 18.5°$), with sharp reflections for ZnO (a curing additive), and a pre-stage of a layer-like super-lattice (at lower scattering angles). The untreated composite represents a superposition of the scattering pattern for both the cured ENR with the reflections from crystalline anhydrite and bassanite, as well. The super-lattice has originated a series of reflections (higher orders of the same layer distance d_L = 5.0 nm). After water treatment, considerable amounts of anhydrite as well as bassanite were converted into gypsum. In addition, there is a series of reflections related to those from anhydrite, bassanite, gypsum, and zinc oxide. The interaction of water with the ENR-$CaSO_4$ composite provokes a strong improvement of the super lattice resulting in very sharp and strong higher order reflections based on a layer distance d_L = 5.0 nm (with odd-even effect). A presentation of the scattering pattern at low angles is shown in Figure 4b as lg(I) vs. lg(d).

In order to make a direct visualization of water-induced structural changes of $CaSO_4$ phase in the elastomer matrix, an additional microscopic analysis was performed. The TEM revealed an agglomerated and irregular shaped $CaSO_4$ structure in the ENR matrix for the untreated composite (Figure 5a). Interestingly, the rod like defined crystal structure (shown by arrow marks in Figure 5b-b') of $CaSO_4$ was developed after the composite had been water-treated. This highly anisotropic crystalline structure with higher aspect ratio of the hydrated particles, when compared with the untreated morphology of the $CaSO_4$ particles, directly corroborates the evidence from the mechanical performance of the composites. The width of this crystal was found to be in the range of 300-400 nm. Formation of this crystal structure has also been

verified using AFM (shown by arrow marks in Figure 5d-d'). The development of a single crystal structure is clearly reflected from the high resolution AFM image (Figure 5d'). Significant improvement in the mechanical, dynamic mechanical and thermal properties of the composites are associated with a significant modification of the water-induced crystal structure of $CaSO_4$ due to an increased aspect ratio of the $CaSO_4$ particles. However, some unreacted $CaSO_4$ was also present after water treatment as shown in Figure 5. This observation is in line with the appearance of a minor Raman bank at 1017 cm^{-1} which correspond to the hemihydrate state of $CaSO_4$. The complete conversion and growth of such hydrated crystal of $CaSO_4$ inside a hydrophobic rubber is quite difficult due to limitation of dimensional space and a limited water absorption capacity.

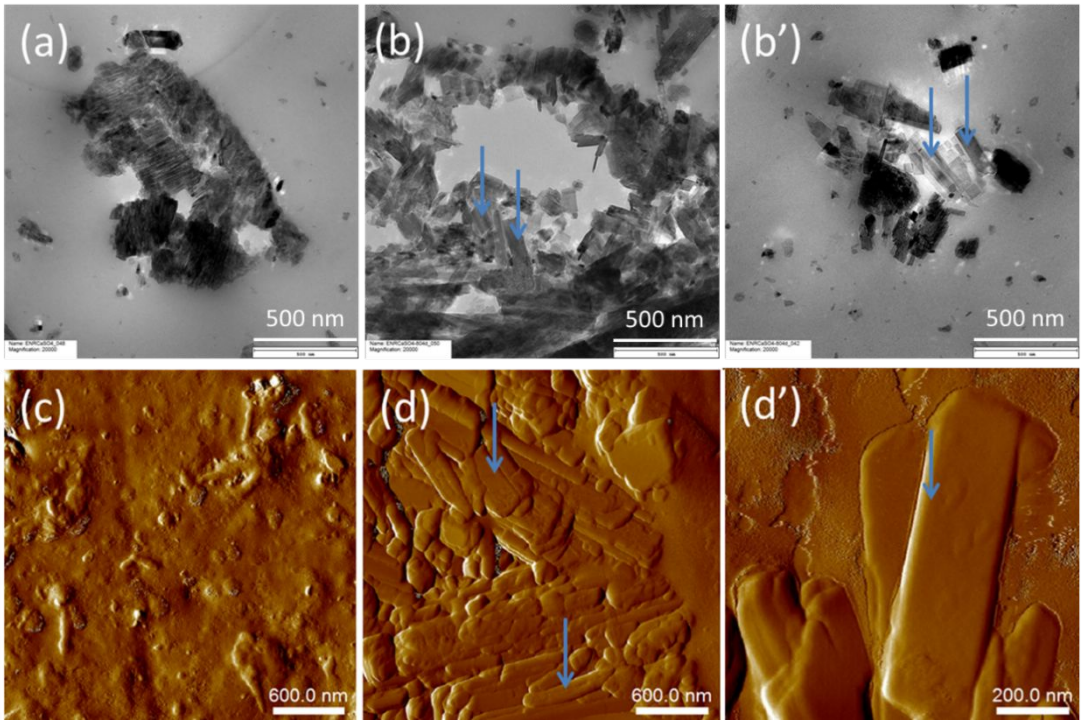

Figure 5. **Transmission electron microscopy images of the (a) untreated and (b-b') water-treated ENR-$CaSO_4$ composites, and atomic force microscopy phase images of (c) untreated and (d-d') water-treated ENR-$CaSO_4$ composites. Rod like crystal structures are shown by the arrow marks.**

Conclusions:

Natural rubber based biomimetic water-responsive elastomeric composites were successfully prepared by using $CaSO_4$ as the water-responsive phase and ENR as an elastomeric matrix. At elevated temperature the water imbibition of ENR enables the development of *in-situ* hydrated crystal structures of $CaSO_4$ in a confined crosslinked ENR matrix. The extent of hydration allows a mechano-adaptable elastomer composite to be developed. The characterization revealed that the water-induced phase transformation process of $CaSO_4$ from non-reinforcing hemihydrate to a reinforcing hydrated crystalline state in the ENR matrix that has a significant influence on the morphology of the composites, which in turn influences the stimuli-responsive properties of the composite, in particular the extent of the mechanical reinforcement and thermal stability. The non-reinforcing and reinforcing abilities of $CaSO_4$ in the elastomer matrix can be altered using an adequate hydration-dehydration process. About a 100 % modulus increase and approximately a 20 °C shift of the thermal degradation temperature was achieved by this process. This simple concept is expected to be applicable to other commercially important elastomers to produce new generation mechanically adaptive polymeric materials. We would like to extend this work to understand whether the reversible transformation of the mechanical properties would be realized by in situ cyclic transformation of the calcium sulphate crystalline structure or not.

Supporting Information

Water absorption capability of filled and unfilled ENR (Figure S1)

Mechano-adaptive properties of unfilled ENR (Figure S2)

Activation energy of the composites (Equation S1)

Acknowledgement

The authors would like to acknowledge Holger Scheibner, Sabine Krause, René Jurk and Uta Reuter from Leibniz-Institut für Polymerforschung Dresden e.V. for executing mechanical, TGA, DMA and TEM experiments, respectively. Authors are thankful to Mrs. Judit Nelke,

IPF Dresden, for providing the graphical abstract. The financial support was received from IPF Annex fund.

References

1. Shanmuganathan, K.; Capadona, J. R.; Rowan, S. J.; Weder, C., Stimuli-responsive mechanically adaptive polymer nanocomposites. *ACS Appl. Mater. Interfaces* **2009,** *2* (1), 165-174.
2. Shanmuganathan, K.; Capadona, J. R.; Rowan, S. J.; Weder, C., Biomimetic mechanically adaptive nanocomposites. *Prog. Polym. Sci.* **2010,** *35* (1), 212-222.
3. Harris, J.; Hess, A. E.; Rowan, S. J.; Weder, C.; Zorman, C.; Tyler, D.; Capadona, J. R., In vivo deployment of mechanically adaptive nanocomposites for intracortical microelectrodes. *J. Neural Eng.* **2011,** *8* (4), 046010.
4. Lobez Comeras, J. M. New functional polymers for sensors, smart materials and solar cells. Ph. D. Dissertation, Massachusetts Institute of Technology, Cambridge, MA, 2012.
5. Mohanty, A. K.; Ghosh, A.; Sawai, P.; Pareek, K.; Banerjee, S.; Das, A.; Pötschke, P.; Heinrich, G.; Voit, B., Electromagnetic interference shielding effectiveness of MWCNT filled poly (ether sulfone) and poly (ether imide) nanocomposites. *Polym. Eng. Sci.* **2014,** *54* (11), 2560-2570.
6. Mcknight, G.; Doty, R.; Keefe, A.; Herrera, G.; Henry, C., Segmented reinforcement variable stiffness materials for reconfigurable surfaces. *J. Intell. Mater. Syst. Struct.* **2010,** *21* (17), 1783-1793.
7. McEvoy, M. A.; Correll, N., Thermoplastic variable stiffness composites with embedded, networked sensing, actuation, and control. *J. Compos. Mater.***2015,** *49* (15), 1799-1808.
8. Kushner, A. M.; Vossler, J. D.; Williams, G. A.; Guan, Z., A biomimetic modular polymer with tough and adaptive properties. *J. Am. Chem. Soc.* **2009,** *131* (25), 8766-8768.
9. Stone, D. A.; Korley, L. T., Bioinspired polymeric nanocomposites. *Macromolecules* **2010,** *43* (22), 9217-9226.
10. Wu, T.; Chen, B., Biomimetic chitosan-treated clay–elastomer composites with water-responsive mechanically dynamic properties. *J. Polym. Sci., Part B: Polym. Phys.* **2014,** *52* (1), 55-62.
11. Bar-Cohen, Y., *Biomimetics: biologically inspired technologies*. CRC Press, Taylor & Francis Group: New York; 2005.
12. Zhu, Y.; Hu, J.; Luo, H.; Young, R. J.; Deng, L.; Zhang, S.; Fan, Y.; Ye, G., Rapidly switchable water-sensitive shape-memory cellulose/elastomer nano-composites. *Soft Matter* **2012,** *8* (8), 2509-2517.
13. Tian, M.; Zhen, X.; Wang, Z.; Zou, H.; Zhang, L.; Ning, N., Bioderived rubber–cellulose nanocrystal composites with tunable water-responsive adaptive mechanical behavior. *ACS Appl. Mater. Interfaces* **2017,** *9* (7), 6482-6487.
14. Murariu, M.; Ferreira, A. D. S.; Degée, P.; Alexandre, M.; Dubois, P., Polylactide compositions. Part 1: Effect of filler content and size on mechanical properties of PLA/calcium sulfate composites. *Polymer* **2007,** *48* (9), 2613-2618.
15. Gorrasi, G.; Vittoria, V.; Murariu, M.; Ferreira, A. D. S.; Alexandre, M.; Dubois, P., Effect of filler content and size on transport properties of water vapor in PLA/calcium sulfate composites. *Biomacromolecules* **2008,** *9* (3), 984-990.
16. Sobkowicz, M. J.; Feaver, J. L.; Dorgan, J. R., Clean and green bioplastic composites: comparison of calcium sulfate and carbon nanospheres in polylactide composites. *CLEAN–Soil, Air, Water* **2008,** *36* (8), 706-713.
17. Freyer, D.; Voigt, W., Crystallization and phase stability of CaSO 4 and CaSO 4–based salts. *Monatsh. Chem.* **2003,** *134* (5), 693-719.
18. Chen, Q.; Jia, C.; Li, Y.; Xu, J.; Guan, B.; Yates, M. Z., α-Calcium sulfate hemihydrate nanorods synthesis: a method for nanoparticle preparation by mesocrystallization. *Langmuir* **2017,** *33* (9), 2362-2369.

19. Musso, S.; Robisson, A.; Maheshwar, S.; Ulm, F.-J., Stimuli-responsive cement-reinforced rubber. *ACS Appl. Mater. Interfaces* **2014,** *6* (9), 6962-6968.
20. Robisson, A.; Maheshwari, S.; Musso, S.; Thomas, J. J.; Auzerais, F. M.; Han, D.; Qu, M.; Ulm, F.-J., Reactive elastomeric composites: When rubber meets cement. *Compos. Sci. Technol.* **2013,** *75*, 77-83.
21. Annamalai, P. K.; Dagnon, K. L.; Monemian, S.; Foster, E. J.; Rowan, S. J.; Weder, C., Water-responsive mechanically adaptive nanocomposites based on styrene–butadiene rubber and cellulose nanocrystals, processing matters. *ACS Appl. Mater. Interfaces* **2014,** *6* (2), 967-976.
22. Natarajan, T. S.; Okamoto, S.; Stöckelhuber, K. W.; Wiessner, S.; Reuter, U.; Fischer, D.; Ghosh, A.; Heinrich, G.; Das, A., In-situ polymorphic alteration of filler structures for biomimetic mechanically adaptive elastomer nanocomposites. *ACS Appl. Mater. Interfaces* **2018**.
23. Natarajan, T. S.; Stöckelhuber, K. W.; Malanin, M.; Eichhorn, K.-J.; Formanek, P.; Reuter, U.; Wießner, S.; Heinrich, G.; Das, A., Temperature-dependent reinforcement of hydrophilic rubber using ice crystals. *ACS Omega* **2017,** *2* (2), 363-371.
24. Panthapulakkal, S.; Sain, M., Studies on the water absorption properties of short hemp—glass fiber hybrid polypropylene composites. *J. Compos. Mater.* **2007,** *41* (15), 1871-1883.
25. Kraus, G., Swelling of filler-reinforced vulcanizates. *J. Appl. Polym. Sci.* **1963,** *7* (3), 861-871.
26. Kissinger, H. E., Reaction kinetics in differential thermal analysis. *Anal. Chem.* **1957,** *29* (11), 1702-1706.
27. Domurath, J.; Saphiannikova, M.; Férec, J.; Ausias, G.; Heinrich, G., Stress and strain amplification in a dilute suspension of spherical particles based on a Bird–Carreau model. *J. Non-Newtonian Fluid Mech.* **2015,** *221*, 95-102.
28. Domurath, J.; Saphiannikova, M.; Heinrich, G., The Concept of hydrodynamic Amplification in filled Elastomers. *Kautsch. Gummi Kunstst.* **2017,** *70* (1-2), 40-43.
29. Shankar Banerjee, S.; Ramakrishnan, I.; Satapathy, B. K., Rheological behavior and network dynamics of silica filled vinyl-terminated polydimethylsiloxane suspensions. *Polym. Eng. Sci.* **2017,** *57* (9), 973-981.
30. Huber, G.; Vilgis, T. A.; Heinrich, G., Universal properties in the dynamical deformation of filled rubbers. *J. Phys.: Condens. Matter* **1996,** *8* (29), L409.
31. Prieto-Taboada, N.; Gómez-Laserna, O.; Martínez-Arkarazo, I.; Olazabal, M. a. A. n.; Madariaga, J. M., Raman spectra of the different phases in the CaSO4–H2O system. *Anal. Chem.* **2014,** *86* (20), 10131-10137.

TOC Graphic

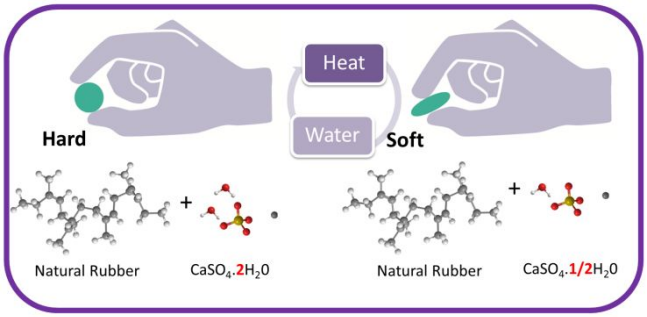
Heat
Water
Hard
Soft
Natural Rubber
$CaSO_4.2H_20$
Natural Rubber
$CaSO_4.1/2H_20$